# Thermoreversible Morphology Transitions of Poly(styrene-*b*-dimethylsiloxane) Diblock Copolymer Micelles in Dilute Solution

**Sayeed Abbas,[†] Zhibo Li,[‡] Hassan Hassan,[‡] and Timothy P. Lodge*[,†,‡]**

*Department of Chemical Engineering and Materials Science and Department of Chemistry, University of Minnesota, Minneapolis, Minnesota 55455*

*Received December 4, 2006; Revised Manuscript Received March 23, 2007*

ABSTRACT: Dilute solutions of a poly(styrene-*b*-dimethylsiloxane) diblock copolymer with block molecular weights of 4 and 12 kDa, respectively, were prepared in a series of styrene-selective dialkyl phthalates: dioctyl phthalate (DOP), dibutyl phthalate (DBP), and diethyl phthalate (DEP). The phthalates were chosen because the interfacial tension between the core block and the solvent can be continuously varied by mixing the solvents in varying proportions. The morphologies were characterized by cryogenic transmission electron microscopy (cryo-TEM) and dynamic light scattering (DLS). By increasing the selectivity of the mixed solvent at room temperature the equilibrium micelle morphology changed from spheres (DOP) to cylinders (DBP) to vesicles (DEP). The selectivity of the solvent was then reduced by increasing the temperature, and we observed the reverse transitions: cylinders → spheres (in DBP) and vesicles → cylinders → spheres (in DEP). Since the core block is always above its glass transition temperature ($T_g \approx -123$ °C), micellar rearrangement was possible within the time scale of the experiment (i.e., minutes). An interesting consequence of these thermotropic transitions is that the viscosity of the solution can be increased upon heating. For example, in the mixed solvent DEP/DBP (1:1), the diblock forms vesicles at room temperature, but when heated, the micelle morphology changes to cylinders and the viscosity of the solution increases by an order of magnitude.

## Introduction

Block copolymers self-assemble into a rich variety of micellar morphologies in selective solvents. The micelle morphology is determined by a free energy balance among the chain stretching in the core, chain repulsion in the corona, and the interfacial tension at the core/corona interface. The morphology can therefore be varied either by tuning the interfacial tension between the solvophobic blocks and the solvent or by varying the composition of the copolymer. Recent reviews on the subject are available.[1,2] Extensive studies on aqueous systems have shown that by increasing the relative proportion of the core block at room temperature, the shape sequence of spheres → cylinders → vesicles can be observed.[3−6] However, there have been relatively few reports on morphological transitions in organic solvents.[7−15] Canham et al. observed the formation of worm-like micelles by dispersing poly(styrene-*b*-butadiene-*b*-styrene) (SBS) in ethyl acetate.[7] Liu et al. established the universal shape sequence of spheres/cylinders/vesicles by dissolving poly(isoprene-*b*-2-cinnamoylethyl methacrylate) in solvents such as cyclopentane.[8−10] Bang et al. also reported the same shape sequence by dissolving poly(styrene-*b*-isoprene) (SI) in mixtures of dialkyl phthalates.[11−13] These authors further demonstrated that small-angle X-ray scattering (SAXS) and cryogenic transmission electron microscopy (cryo-TEM) can be utilized to characterize such systems in detail. LaRue et al. dissolved SI diblock copolymers in heptane, a polyisoprene (PI) selective solvent, and showed that morphological shape transitions can also be observed by increasing temperature.[14,15] The authors also observed that the morphology was recovered upon cooling and hence concluded that the transitions were reversible. However it took days for the original morphology to be recovered. This observation can be rationalized by noting that the glass transition temperature ($T_g$) of the core block was higher than the temperatures at which the experiments were performed. The results of the experiments were further used to test a detailed model of micellization of diblock copolymers in selective solvents.[16]

In this paper we report the formation of micelles by dissolving poly(styrene-*b*-dimethylsiloxane) (SD) in dialkyl phthalates: dioctyl phthalate (DOP), dibutyl phthalate (DBP), and diethyl phthalate (DEP), of which DEP is the most selective for polystyrene. The selectivity of the solvent can be varied by mixing the different phthalates. There are several advantages of choosing this system. First, the $T_g$ (−123 °C) of polydimethylsiloxane (PDMS) core block is much less than room temperature, and hence there is no dynamic barrier for chain transfer motion within the core. Second, the interfacial tension between PDMS and the dialkyl phthalates is large, and thus the thermotropic transitions are well defined. For example in DEP we observe the entire phase sequence of vesicle → cylinder → sphere in a single solvent. Moreover, very long cylindrical micelles are formed in solution, which leads to significant modification in the viscosity of the solvent. Finally, sufficient electron density difference exists between PDMS and the phthalates to enable the use of cryo-TEM to characterize the samples. We have also used dynamic light scattering to estimate the dimensions of the micelles and rheology to measure the viscosity of the solutions.

## Experimental Section

**Materials.** An SD diblock copolymer with block molecular weights of 4 and 12 kDa, respectively, was synthesized by anionic polymerization. All the monomers were obtained from Sigma-Aldrich and were purified by stirring over dibutyl magnesium for 4 h to remove traces of moisture before reaction. Hexamethylcyclotrisiloxane ($D_3$) was stirred at 90 °C since it is a solid at room

* Author for correspondence. E-mail: lodge@chem.umn.edu.
[†] Department of Chemical Engineering and Materials Science.
[‡] Department of Chemistry.

10.1021/ma062779o CCC: $37.00 
Published on Web 04/28/2007

temperature. Reaction was initiated by adding *sec*-butyl lithium to styrene monomer dissolved in cyclohexane and was allowed to proceed for 4 h at 40 °C, after which the second monomer ($D_3$) was added. The solution was stirred overnight at 25 °C, after which tetrahydrofuran (THF) was added so that the solution had cyclohexane and THF in equal proportions. After allowing the reaction to proceed for a further 90 min it was terminated by adding excess trimethylchlorosilane. The product after reaction was washed with 5% $NaHCO_3$, followed by repeated water washes. The polymer was recovered by precipitation in a 50/50 mixture of methanol and 2-propanol. The molecular weight of the diblock was measured by a combination of size exclusion chromatography (SEC) and nuclear magnetic resonance spectroscopy ($^1$H NMR). The number average molecular weight of the PS (first block) was measured by SEC equipped with both refractive index (Wyatt Optilab) and light scattering (Wyatt Dawn) detectors. The block composition was determined from $^1$H NMR spectroscopy, following which the molecular weight of PDMS (second block) was determined. The polydispersity index of the polymer was measured by SEC to be 1.09. All the solvents were purchased from Sigma Aldrich and were used without any further purification. Dilute solutions (1 wt %) of the diblock were prepared by dissolving the polymer in phthalates using a cosolvent (methylene choloride). The cosolvent was later removed by evaporation until constant weight was achieved. Henceforth the diblock will be referred to as SD(4−12).

**Cryogenic Transmission Electron Miscroscopy.** Cryo-TEM was performed to characterize the morphology of the micelles. A small droplet of solution was placed on a holey carbon film, which was further supported on a TEM copper grid. The droplet was then blotted to form a film of solution on the grid and allowed to equilibrate. The sample-loaded grid was then plunged into liquid nitrogen, and the solvent was vitrified. The sample was then transported under liquid nitrogen and mounted onto the cryo holder of the TEM. During the entire measurement, the sample was under vacuum. All the images were acquired in a JEOL 1210 TEM, operating at 120 kV and equipped with a Gatan 626 cryo holder. The temperature of the sample was maintained at −178 °C. A Gatan multiscan 724 digital camera was used to record the images, which were then processed using DigitalMicrograph software.

**Dynamic Light Scattering.** The variation of the size of the micelles as a function of temperature was measured by dynamic light scattering (DLS). To avoid dust in the samples, the solution was filtered through 0.2 $\mu$m filters and then flame sealed in 0.25 in. tubes to avoid solvent evaporation. The DLS instrument is composed of a home-built goniometer, an electrically heated silicon oil bath, a Brookhaven BI-DS photomultiplier, a Lexel 95-2 Ar+ laser operating at 488 nm, and a Brookhaven BI-9000 correlator. The intensity autocorrelation functions were measured at three angles (60°, 90°, and 120°). The function was fitted to the cumulant expression from which the decay constant ($\bar{\Gamma}$) and second moment about $\bar{\Gamma}$ ($\mu_2$) was obtained.[17] The Stokes−Einstein equation was then used to calculate the average hydrodynamic radius of the micelles from $\bar{\Gamma}$. We also calculated the polydispersity of the micelles ($\bar{\Gamma}/\mu_2^2$) to estimate the width of the size distribution.

**Rheology.** Steady shear flow was used to measure the viscosity of the solutions. The experiments were performed on a Rheometrics fluids spectrometer (RFS-II) with a 34 mm diameter couette cup (stator) and a 32 mm diameter cylindrical bob (rotor). The temperature was controlled by a circulating water/ethylene glycol bath. The nonlinear rheology of worm-like micelles was studied by conducting shear rate sweep experiments on the solutions. The viscosity of the pure solvents was also measured as a function of temperature, and the obtained data were used in calculations of micelle dimensions via the Stokes−Einstein equation.

## Results and Discussions

**Phase Sequence at Room Temperature.** At room temperature the full sequence of spheres, cylinders, and vesicles was observed with increasing solvent selectivity. The interfacial tension between the core block and the solvent was varied by mixing different proportions of the solvents. Dioctyl phthalate (DOP) is the least selective whereas diethyl phthalate (DEP) is the most selective solvent. Thus a solvent intermediate in selectivity for PS can be prepared by blending DOP and DEP. Cryo-TEM was performed on the samples to identify the morphology of the micelles. Representative images of the spheres (DOP), cylinders (DBP), and vesicles (DEP) observed in the system are shown in Figure 1.

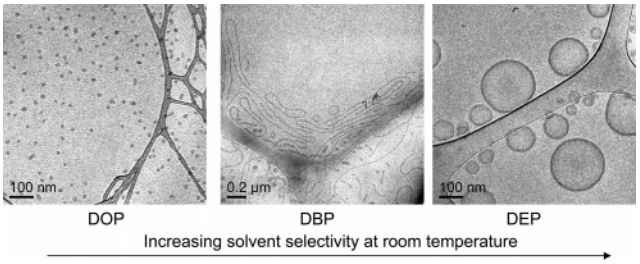


**Figure 1.** Cryo-TEM images showing the existence of spheres, cylinders, and vesicles in DOP, DBP, and DEP, respectively. All the samples were quenched from room temperature.

The key aspect that should be noted here is that the morphological transitions are observed for a single diblock whose volume fraction ($f_{PS}$) of PS is 0.24. Previously, extensive work has been done on SI block copolymers in phthalates, but over the composition range of $0.23 < f_{PS} < 0.7$ only spheres were observed.[18,19] With $f_{PS} \approx 0.16$ prolate ellipsoidal micelles were reported,[20] and finally with $f_{PS} \approx 0.15$, the full morphological transitions were observed with increasing solvent selectivity.[13] In a PI selective solvent and with PS in the core, LaRue et al. observed cylinders at $f_{PI} \approx 0.25$ and vesicles at $f_{PI} \approx 0.19$.[15]

In this study, we observe vesicles at $f_{PS} \approx 0.24$. Consistent with this, the critical micellization temperatures (CMT) are systematically higher than the SI system previously studied. These observations are the result of higher interfacial tension between PDMS and the phthalates. For example, the interaction parameter at room temperature (estimated from solubility parameters) between PDMS and DEP ($\chi_{PDMS-DEP}$) is 2.3, whereas $\chi_{PI-DEP}$ is 1.2. The higher CMT of SD + phthalate also allows us to explore thermotropic transitions, which will be discussed in the next section. The high interfacial tension also leads to the formation of very long cylinders (almost on the order of 1 $\mu$m), which can ultimately lead to significant modification of the solution viscosity.

**Thermotropic Transitions.** The thermotropic transitions were observed by measuring the change in hydrodynamic size ($R_h$) of the micelles with temperature. The amount of time devoted for annealing the samples after each temperature change was 15 min. Both heating and cooling ramps were performed to study the reversibility of the transitions. Figure 2 shows the results from a 1% solution of SD(4−12) in DBP. At room temperature the diblock formed cylindrical micelles, but as the temperature was increased, the $R_h$ of the nanoaggregates decreased, indicating a change in micelle morphology. The transition was gradual, and for $T > 70$ °C there was little further change in $R_h$, from which we can conclude that the transformation to spheres is complete at 70 °C. From these data we infer that as the temperature goes up and solvent selectivity goes down, the average cylinder becomes progressively shorter. This happens because the energetic penalty to have cylinder end caps decreases, thereby reducing the length of cylinders in solution. Finally there is a state of coexistence where both spheres and

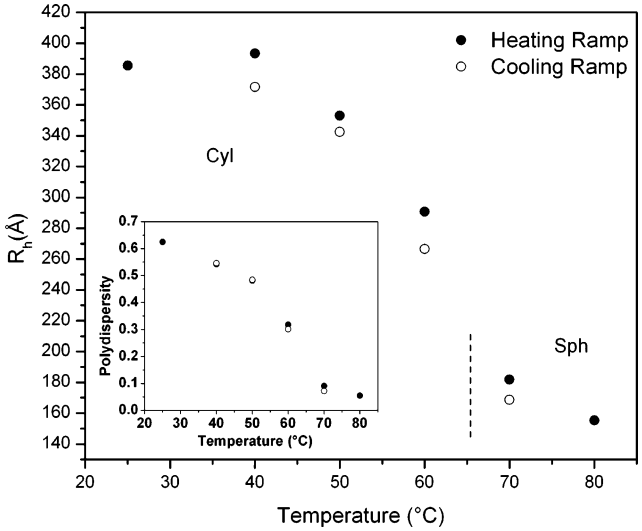


**Figure 2.** Variation of hydrodynamic radius ($R_h$) as a function of temperature for a 1% solution of SD(4−12) in DBP. The dotted line indicates the transition temperature. The inset shows the change in polydispersity of the micelles during the same heating and cooling ramps.

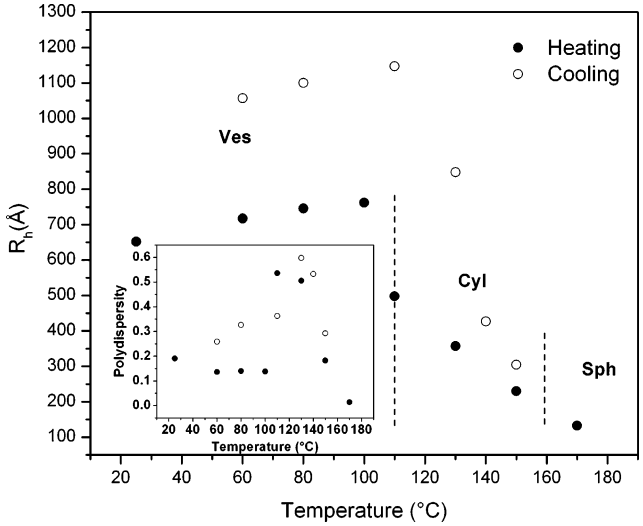


**Figure 3.** Variation of hydrodynamic radius ($R_h$) as a function of temperature for the sample 1% solution of SD(4−12) in DEP. The dotted lines indicate the transition temperatures. The inset shows the change in polydispersity of the micelles during the same heating and cooling ramps.

cylinders are present. On further increase in temperature, the cylinders totally disappeared. The $R_h$ of the micelles during the cooling ramp followed the same trend as the heating ramp, from which we can conclude that the cylinder → sphere transition is completely reversible on this time scale. The inset in Figure 2 shows the variation of polydispersity of the micelles during the same heating and cooling ramps. The cylinders are highly polydisperse at room temperature, but with increase in temperature, the polydispersity decreases. After the cylinder → sphere transition ($T > 70$ °C), we observe that the polydispersity remains unchanged at low values, thus indicating that the spherical micelles have a narrow size distribution. The change in $R_h$ and polydispersity during the heating and cooling ramps shows remarkable similarity with each other and hence further reinforces the conclusion that we are observing a thermoreversible change in micelle morphology in a time scale of minutes.

When the selectivity of the solvent was further increased by using diethyl phthalate as the selective solvent, vesicles are formed. Figure 1 shows a cryo-TEM image of the 1% solution of SD(4−12) in DEP. When the solution was heated, the full sequence of vesicles → cylinders → spheres was observed in a single sample. Figure 3 shows the change in $R_h$ of the sample with temperature on heating and cooling. At 110 °C there was an abrupt drop in the $R_h$ of the micelles, indicating a change in the morphology from vesicles to cylinders. On further heating the $R_h$ decreased gradually and became almost constant at 160 °C, thereby suggesting another change. If we compare the heating curve in Figure 3 above 110 °C to that of the heating curve in Figure 2, we see a strong similarity between the two. The similarity of the curves suggests that the second transition in Figure 3 is the cylinder → sphere transition. This is also supported by the magnitude of $R_h$ above 160 °C; the value of ca. 130 Å coincides well with those for spheres in Figure 2. We again observed that in the cooling ramp the cylinder → sphere transition was reversible, but during the vesicle → cylinder transition, the mean value of $R_h$ of the heating and cooling ramps exhibited hysteresis; the location of the transition itself did not change. The sample was annealed for 2 h at 110 °C (during the cooling ramp), but no significant change was observed in $R_h$. This indicates an interesting difference in the mean vesicle size, depending on preparation history. Those formed on cooling from cylinders are larger than those formed upon dissolution with a cosolvent. We speculate that the larger vesicles are closer to the equilibrium size, as the original vesicles were formed in a mixed solvent of lower interfacial tension. On the other hand, as noted below, the vesicles formed from the cylinders have a broader size distribution. In comparison Larue et al. showed that upon heating, 18 h were required for the cylinder → sphere transition, whereas on quenching, the sphere → cylinder transition was not complete even after annealing for 36 days.[15] The results indicate that a glassy core significantly hampers dynamic chain exchange between micelles and can increase the time required to reach thermodynamic equilibrium. In the SD + dialkyl phthalate system we have a nonglassy core and all the transformations are thermoreversible.

The inset in Figure 3 also shows the change in polydispersity of the micelles during the same heating and cooling ramps. At 110 °C an abrupt increase in polydispersity occurred, indicating the vesicle → cylinder transformation. From this result we conclude that although the average $R_h$ of the vesicles is larger than the cylinders, the cylinders have a broader size distribution than the vesicles. Above 110 °C, the trend is again similar to what we had observed in Figure 2. During the cooling ramp we again observe hysteresis in polydispersity during the cylinder → vesicle transformation. The vesicles obtained after the cooling ramp have a much higher polydispersity than the vesicles at room temperature (before temperature ramp was started). The general observation that the polydispersity of the cylinders is greater than that of the vesicles, which is greater than that of the spheres, is readily understood. First, for a given variation in micelle aggregation number $Q$, the hydrodynamic radius varies roughly as $Q$, $Q^{1/2}$, and $Q^{1/3}$ for cylinders, vesicles, and spheres, respectively. Therefore ($\partial R_h/\partial Q$) is largest for cylinders. Second, the only energetic consideration in the growth of cylinders is the prevalence of end caps, which leads to a very broad (exponential) distribution in length.[21,22] Spheres, on the other hand, have a rather tightly prescribed optimum $Q$ due to the free energy balance identified in the Introduction. Vesicles are an intermediate case, in that the curvature of the bilayer, which dictates the optimum size, is relatively weakly dependent on $Q$.

It is well established that formation of cylindrical micelles can significantly increase the viscosity of the solution.[22−24] In

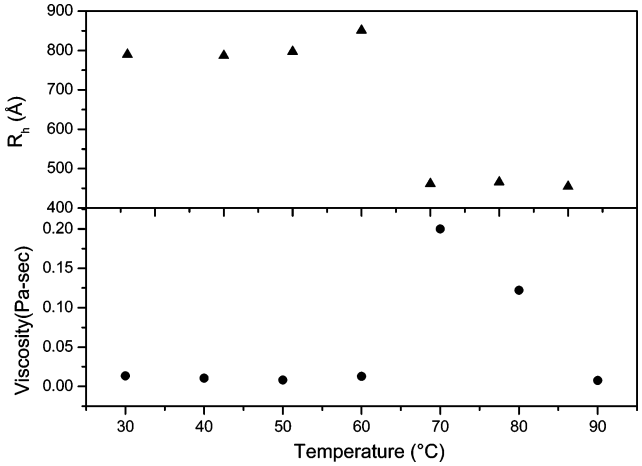


**Figure 4.** Change in $R_h$ of the micelles and viscosity of the sample 1% solution of SD(4−12) in DEP/DBP (1:1) as a function of temperature.

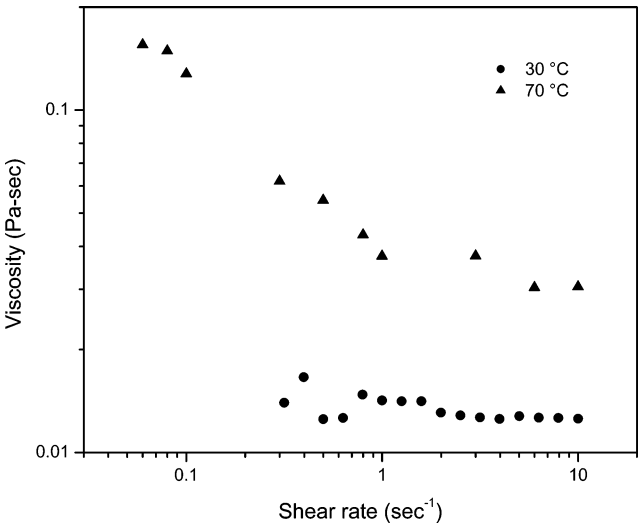


**Figure 5.** Response of a 1% solution of SD(4−12) in DEP/DBP (1:1) to shear rate sweep experiments. At high temperature (70 °C) the solution is shear thinning, whereas at low temperature it is Newtonian.

our system worm-like micelles were formed with increase in temperature; hence we expect the viscosity of the polymer solution to rise, whereas the viscosity of the pure solvent drops with temperature. An example of this phenomenon has been reported for low molecular weight surfactants in water.[25,26] We observe a similar viscosity enhancement with increasing temperature in 1% solution of SD(4−12) in DEP/DBP (1:1). In this sample the solvent is a 1:1 mixture of DEP and DBP and the solvent selectivity lies somewhere between DEP and DBP. Cryo-TEM (data not shown) showed the presence of primarily vesicles in the solution at room temperature. Both the viscosity of the solution and $R_h$ of the micelles were measured as a function of temperature and are shown in Figure 4.

We observed that the increase in viscosity and the drop in $R_h$ of the micelles coincide, and hence we can infer that the formation of cylindrical micelles is responsible for the significant rise in the viscosity of the solution. As shown in Figure 5, at high temperature (70 °C) the sample showed significant shear thinning, whereas at low temperature (35 °C) Newtonian behavior was observed. The shear thinning is characteristic of dilute, long worm-like micelles, whereas vesicle solutions are known to behave as Newtonian fluids.[5] We must state here that adequate precautions were exercised to measure the viscosity of long cylindrical micelles. Cylindrical or worm-like micelles

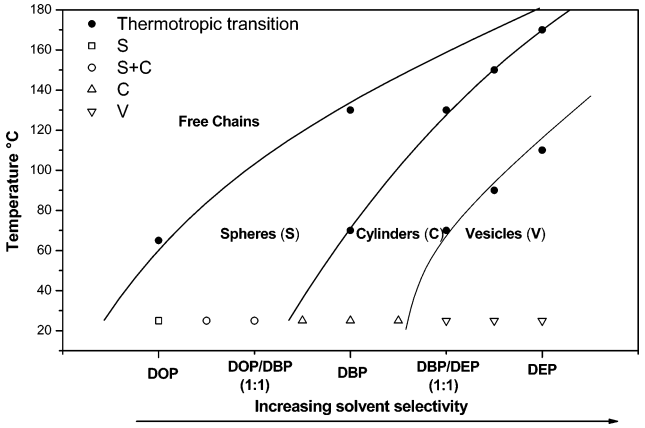


**Figure 6.** Morphology diagram of SD(4−12) in dialkyl phthalates. The solid points are results obtained from DLS measurements and indicate thermotropic transitions. The lines have been drawn through them as a guide to the eye indicating the locus of transitions. Room-temperature cryo-TEM data have been plotted as open symbols.

undergo shear-induced orientation, which can significantly alter the rheology of the solution.[24] A way of observing the structural inhomogeneity is by conducting transient studies on the solution.[27] We monitored the viscosity at the onset of steady shear and accounted for the time the solution takes to reach steady state. It took about 5 min at the lowest shear rate to attain steady state. The viscosities reported in Figure 5 are the steady-state viscosities of the solution at each shear rate.

Based on all the DLS, rheology, and cryo-TEM measurements (some not shown) a morphology diagram was constructed and has been shown in Figure 6. The transitions are broad due to the coexistence of two morphologies near the transition; however, we provide lines as a guide to the eye indicating the locus of transitions. The sequence of transitions observed at room temperature is similar to previous work done in aqueous systems.[5] For example in aqueous solutions of polybutadiene-*b*-polyethylene oxide (PB-PEO) the weight fraction of PEO was varied and the same micelle sequence was observed.[6] The same results were also obtained from extensive studies performed in the polystyrene-*b*-polyacrylic acid (PS-PAA) system in water.[28] In that study both the PS and PAA blocks were varied to change the volumetric composition of the diblock copolymer. Hence we can conclude that the sequence of spheres → cylinders → vesicles is universal, and it can be recovered by altering the thermodynamic interactions between the blocks and the solvent.

## Summary

In this paper we have investigated the micellization behavior of SD(4−12) in pure dialkyl phthalates and their mixtures. When the solvent selectivity was increased, the expected sequence of transitions from spheres to cylinders to vesicles was observed. The reason for the morphological transitions is that when the solvent becomes more selective, the increasing interfacial tension forces the interface to reduce its curvature. Spheres have the highest interfacial curvature, whereas bilayers (or vesicles) have the lowest; hence the sequence of spheres → cylinders → vesicles is observed. Due to the high interfacial tension between PDMS and DBP, we saw the formation of very long cylinders in solution. We also studied morphological transitions as a function of temperature. As the temperature was increased, the selectivity of the solvent decreased. Therefore we observed the reverse sequence of morphological transitions (vesicles → cylinders → spheres). In the time scale of the experiments (15 min) all the transitions were completely reversible. We attributed this to the fact that the glass transition temperature of the core

block was well below the measurement temperatures, which helped in equilibration of the samples. The cylinder → vesicle transition did show hysteresis in that the vesicles did not recover their original $R_h$ values. The transformation from vesicles to cylinders was particularly interesting because it led to a viscosity increase with increasing temperature, due to the formation of long cylinders in solution. A morphology diagram of SD(4−12) in dialkyl phthalates was constructed from the experimental data. The results indicate that the universality of the micelle sequence is dependent only on the thermodynamic interactions between the solvent and the blocks present in the copolymer. We can change the interactions either by changing the identity of the solvent or by changing the temperature, and the same sequence is revealed. The ability to increase solution viscosity on heating via a micelle shape transition may have applications in, for example, lubrication oils.

**Acknowledgment.** This work was supported by the MRSEC Program of the National Science Foundation under Award No. DMR-0212302.

**Supporting Information Available:** Analysis of DLS measurements by cumulant method. This material is available free of charge via the Internet at http://pubs.acs.org.

## References and Notes

(1) Riess, G. *Prog. Polym. Sci.* **2003**, *28*, 1107−1170.
(2) Hamley, I. W. *Block Copolymers in Solution: Fundamentals and Applications*; John Wiley & Sons, Ltd.: Chichester, 2005.
(3) Alexandridis, P., Lindman, B., Ed. *Amphiphilic Block Copolymers: Self-Assembly and Applications*; Elsevier: Amsterdam, 2000.
(4) Zhang, L.; Eisenberg, A. *Science (Washington, D. C.)* **1995**, *268*, 1728−1731.
(5) Won, Y.-Y.; Brannan, A. K.; Davis, H. T.; Bates, F. S. *J. Phys. Chem. B* **2002**, *106*, 3354−3364.
(6) Jain, S.; Bates, F. S. *Science (Washington, D. C.)* **2003**, *300*, 460−464.
(7) Canham, P. A.; Lally, T. P.; Price, C.; Stubbersfield, R. B. *J. Chem. Soc., Faraday Trans. 1* **1980**, *76*, 1857−1867.
(8) Ding, J.; Liu, G. *Macromolecules* **1997**, *30*, 655−657.
(9) Tao, J.; Stewart, S.; Liu, G.; Yang, M. *Macromolecules* **1997**, *30*, 2738−2745.
(10) Ding, J.; Liu, G.; Yang, M. *Polymer* **1997**, *38*, 5497−5502.
(11) Lodge, T. P.; Bang, J.; Li, Z.; Hillmyer, M. A.; Talmon, Y. *Faraday Discuss.* **2004**, *128*, 1−12.
(12) Kesselman, E.; Talmon, Y.; Bang, J.; Abbas, S.; Li, Z.; Lodge, T. P. *Macromolecules* **2005**, *38*, 6779−6781.
(13) Bang, J.; Jain, S.; Li, Z.; Lodge, T. P.; Pedersen, J. S.; Kesselman, E.; Talmon, Y. *Macromolecules* **2006**, *39*, 1199−1208.
(14) LaRue, I.; Adam, M.; da Silva, M.; Sheiko, S. S.; Rubinstein, M. *Macromolecules* **2004**, *37*, 5002−5005.
(15) LaRue, I.; Adam, M.; Pitsikalis, M.; Hadjichristidis, N.; Rubinstein, M.; Sheiko, S. S. *Macromolecules* **2006**, *39*, 309−314.
(16) Zhulina, E. B.; Adam, M.; LaRue, I.; Sheiko, S. S.; Rubinstein, M. *Macromolecules* **2005**, *38*, 5330−5351.
(17) Koppel, D. E. *J. Chem. Phys.* **1972**, *57*, 4814−4820.
(18) Hanley, K. J.; Lodge, T. P.; Huang, C.-I. *Macromolecules* **2000**, *33*, 5918−5931.
(19) Lodge, T. P.; Pudil, B.; Hanley, K. J. *Macromolecules* **2002**, *35*, 4707−4717.
(20) Pedersen, J. S.; Hamley, I. W.; Ryu, C. Y.; Lodge, T. P. *Macromolecules* **2000**, *33*, 542−550.
(21) Marques, C. M.; Cates, M. E. *J. Phys. II* **1991**, *1*, 489−492.
(22) Cates, M. E.; Candau, S. J. *J. Phys.: Condens. Matter* **1990**, *2*, 6869−6892.
(23) Candau, S. J.; Oda, R. *Colloids Surf. A* **2001**, *183*, 5−14.
(24) Berret, J. F. In *Molecular Gels: Materials with Self-Assembled Fibrillar Networks*; Weiss, R. G., Terech, P., Eds.; Springer: Amsterdam, 2006.
(25) Kalur, G. C.; Frounfelker, B. D.; Cipriano, B. H.; Norman, A. I.; Raghavan, S. R. *Langmuir* **2005**, *21*, 10998−11004.
(26) Hassan, P. A.; Valaulikar, B. S.; Manohar, C.; Kern, F.; Bourdieu, L.; Candau, S. J. *Langmuir* **1996**, *12*, 4350−4357.
(27) Shikata, T.; Hirata, H.; Takatori, E.; Osaki, K. *J. Non-Newton. Fluid* **1988**, *28*, 171−182.
(28) Zhang, L.; Eisenberg, A. *Polym. Adv. Technol.* **1998**, *9*, 677−699.

MA062779O